N74-34580

PLASMA SPECTROSCOPY USING THE SHOCK TUBE AS A LIGHT SOURCE

BY

T. D. WILKERSON AND M. H. MILLER

Plasma Spectroscopy Using the Shock Tube as a Light Source

T. D. WILKERSON AND M. H. MILLER

Abstract—Measurement of optical properties of plasmas is described as an important application of the gas-driven shock tube. The electrical engineering context is the study and application of plasmas having temperatures of order 1eV (11 600°K) for which both atomic and collective properties need to be known.

The gas driven shock tube heats samples of gas to temperatures of 9000–13 000°K at total pressures of 10–20 atm. Steady state conditions during which the gas is in collisional thermal equilibrium persist for 100–200 μs. Spectral line emission (e.g., H, C, C^+, P, P^+, Fe, Fe^+, O, U, U^+, U^{++}) and continuum radiation are correlated with the measured thermodynamic state of the gas to obtain either absolute transition probabilities, Stark broadening, and Stark shift parameters for the particular lines, or complete tabulations of optical depth versus wavelength for complex and incompletely classified spectra.

The atomic data, as well as some newly developed spectroscopic techniques, facilitate the measurement of composition, temperature, pressure, and electron density in high temperature plasma devices. Measured optical depths of uranium plasmas already directly test predictions vital to the design of proposed, gas-core fission reactors.

I. INTRODUCTION

ABOVE the pyrometric temperature range (1000–3000°K) characteristic of flames and furnaces, modern technology has increasingly explored the 10 000°K range for purposes of energy conversion and propulsion. Though the designs of the corresponding practical devices are not yet entirely clear, these higher temperatures (~ 1 eV) offer potential advantages for specific impulse, electrical conductivity, and cycle efficiency. Examples are magnetohydrodynamic (MHD) power generators and propulsion devices based on the gas-core nuclear reactor. Bulk plasmas at even higher temperatures, say 10–100 eV, may be required for the optimal mediation between fusion and fission energy sources and the requisite temperatures of any exhaust system.

As well as electrons, such plasmas contain atoms and ions, significant fractions of which are excited and emit light. The emission spectra are usually mixtures of continuum radiation, due to free–free and free–bound electron transitions, and line radiation from atoms and ions; the relative intensities and the shapes of the spectral lines

depend on the chemical composition, temperature, and density of the plasma.

Given sufficiently comprehensive atomic information, the engineer or physicist can utilize spectroscopy to great advantage in measuring the plasma state so that it can be correlated with such macroscopic observables as the gain in a laser cavity or the electrical conductivity of a plasma jet. Thus today's plasma engineer has a close kinship with the astrophysicist who likewise uses spectroscopic observations to infer the conditions in a gaseous nebula or stellar atmosphere.

Fundamental to such research are the aforesaid atomic data which have often proved difficult to calculate accurately from first principles. Hence the need for controlled light sources operating at $10\,000°K$ and above, in which the composition, temperature, and electron density are known, and whose emission and absorption spectra can therefore be quantitatively interpreted in terms of 1) atomic transition probabilities for the atoms and ions of interest, and 2) broadening parameters for these lines in the plasma environment. Also from an engineering standpoint there are complex cases of practical interest, such as the uranium plasma, where a useful catalogue of emissivity versus wavelength can be sometimes usefully obtained without regard to atomic details. Such data may, in fact, be essential for the engineering design of uranium plasma devices in which radiative transfer directly couples the fuel to the working fluid. On the other hand, the physicist and astrophysicist may be the most interested in using quantitative results of types 1) and 2) above as a test of theory, so as to be able to extrapolate reliably to atomic species or to plasma conditions not directly measured in the laboratory.

The shock tube is a very useful device for establishing a wide range of plasma conditions so that basic physics and engineering data can be obtained under known conditions of temperature, pressure, and electron density. Such research with a gas-driven shock tube is the subject of this paper. Much the same techniques apply to other thermal light sources, such as the wall-stabilized arc and the electrical shock tube. The gas driven shock tube offers the advantages of a large volume of homogeneous conditions and ease of variation of parameters, while it is more transient in character than a dc arc and is generally a lower temperature device than an electrical shock tube.

II. Shock Tube Operation

The main features of shock tube flow are illustrated in Fig. 1. The double compression of gas near the end of the tube is accomplished by the primary and reflected shock waves, leaving a nearly stationary gas sample for observation at conditions p_2, T_2 for times of order $100\,\mu s$. This gas is our controlled light source. In the Maryland shock tube, pressure and temperature behind the reflected shock usually lie in the ranges 10–20 atm and 9000–13 000°K; this gas is uniform over the $7.6\,cm \times 10\,cm$ cross section of the tube, except for $\sim 1\,mm$ thick boundary layers on the walls which usually have no observable effect on the spectra emitted by the gas. This uniformity is due to planarity of the first two shock waves and the thinness of the primary
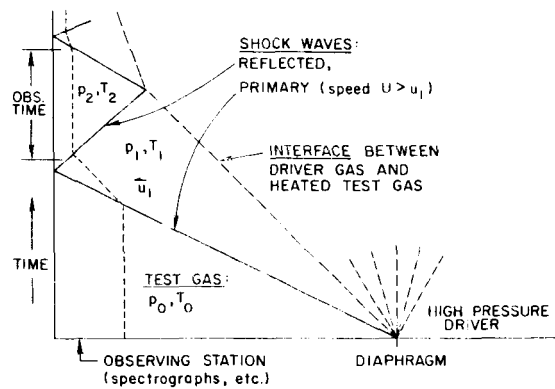

Fig. 1. Distance–time diagram of wave and fluid motion in a gas-driven shock tube. Dotted line (left) shows stepwise compression of gas sample by successive shockwaves.

flow boundary layer. The idealized interface shown is usually not so well defined, so also the subsequent shocks; hence the later, *multiply*-compressed regions (above region 2 on Fig. 1) are used as light sources only for limited spectroscopic data up to 30 atm pressure and 15 000 K.

Under usual operating conditions, region 2 equilibrates in 1–$10\,\mu s$; this is evidenced by the steadiness of light emission and by both experimental and theoretical checks that the steady gas is in local thermodynamic equilibrium (LTE). Roughly speaking, LTE is allowed in dense plasmas of laboratory dimensions both by high self-absorption in the resonance lines of atoms (providing a high rate of transition between ground and excited states) and by large inelastic electron cross sections for excited states (providing a high transition rate *among* the excited atomic states including the unbound states of the ionization continuum).

Given the conditions p_2, T_2 and the known composition of the test gas (e.g., 1 percent PH_3 in neon or $\frac{1}{2}$ percent $H_2 + \frac{1}{2}$ percent UF_6 in neon), the entire thermodynamics of the gas under study can be calculated. This is now based on direct observations of p_2 and T_2, (and for the purposes of redundancy, n_e, the density of free electrons) whereas it used to be done from the Rankine–Hugoniot equations for the primary and reflected shocks, using the observed primary shock speed U. The former is preferable [1], [2] owing to small random and systematic departures of shock tube flow fields from the idealizations inherent in the theory.

Typically, all molecules are dissociated under our conditions; most neutral atoms are at least partially ionized, with each the degree depending on the ionization potential, so that neon (I.P. = 21.56 eV) is ionized only up to about 0.1–0.3 percent in the one extreme while, in the other, the dominant uranium (I.P. = 6.5 eV) species are U^+ and U^{++} (UII and UIII in customary spectroscopic notation). Electron densities are in the range 2×10^{16}–$3 \times 10^{17}\,cm^{-3}$; neon particle densities are in the range 5×10^{18}–$2 \times 10^{19}\,cm^{-3}$. The observed spectra consist primarily of the *lines of neutral and ionized atoms* (particularly the neutral lines showing evidence of Stark broadening and shift due to the charged particles in the plasma) and the *continuum radiation* arising from free–free and free–bound electron transitions in ion fields.

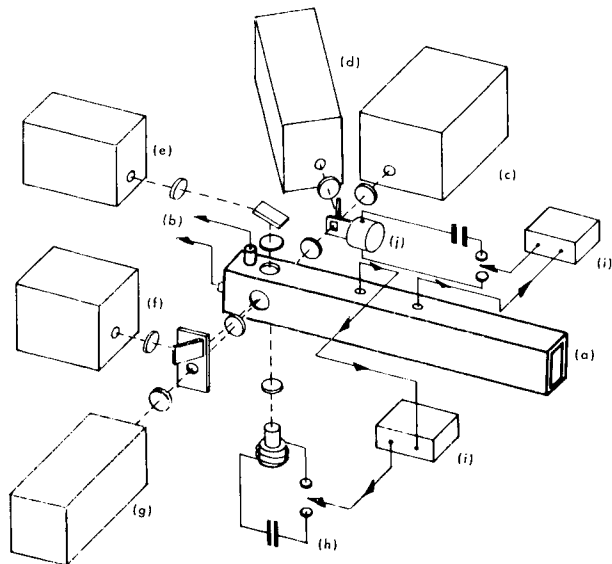Fig. 2 summarizes the "diagnostics" used near the reflec-

Fig. 2. Diagram of apparatus showing location of instruments: (a) Shock tube cross section. (b) Quartz pressure transducers. (c) Medium-resolution spectrograph. (d) High resolution spectrograph. (e) Photoelectric monochromator for reversal measurement. (f), (g) Photoelectric spectrographs. (h) Reversal flash lamp. (i) Delay pulsers for firing flash lamp and shutter from ionization gauges on shock tube. (j) Exploding-wire shutter.
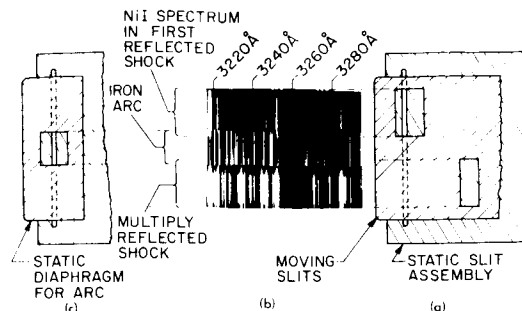

Fig. 3. Typical data obtained by the shutter and a stigmatic (f/9) spectrograph: (a) Slider used to frame sequentially observed shock tube plasmas. (b) Spectrum of nickel in the plasma behind first-reflected and multiply-reflected shocks. (c) Mask used to expose the iron arc fiduciary spectrum.

tion end of the shock tube, including quartz pressure transducers, photoelectric and photographic spectrographs, and ionization gaps for obtaining time-of-arrival signals from the primary shock wave. Such signals are sometimes used for shock speed measurement, but are always needed to trigger the line-reversal flash lamp, the pulsed shutter, and CRO sweeps for all data channels (usually, about 20 in number). Previous descriptions have been given of the radiation-calibration methods [2], [3] and the design and operation of the pulsed shutter [4]; reports are available on the computer codes used for calculating the thermodynamics of the shock tube plasma [5] and for reducing the photographic spectra to absolute intensity versus wavelength [6].

The reader may be particularly interested in the pulsed shutter [4] and in a technique of combining independent radiation measurements so as to obtain atomic transition probabilities which are relatively free from systematic error [1], [7].

III. PULSED SHUTTER

Pulsed shutter operation is illustrated by Fig. 3. A slider containing various apertures is driven at high speed across the slit of a stigmatic spectrograph; the slider is driven by the explosion pressure from an electrically exploded wire [4]. On a single spectrographic plate we record the emission spectra from 8–10 shock tube experiments. Each band of exposure has the appearance of the photographic portion of Fig. 3. A stationary aperture allows us to photograph the central iron-arc spectrum for calibrating the transverse distance scale in terms of wavelength. The slider, owing to the location and size of the apertures and the time of triggering the exploding wire, exposes the upper part of the slit (and therefore the exposure band) to light from behind the first

reflected shock, while the lower part is exposed later to light emitted from the multiply-reflected shock plasma already mentioned in reference to Fig. 1. Thus one exposure band on the plate suffices to observe two sets of physical conditions with as wide a band in wavelength as the spectrograph was designed for, also with the full resolution of which the spectrograph is capable. Commonly, two spectrographs are serviced by a single shutter, as indicated in Fig. 2, one covering 1700 Å with 0.25 Å resolution and the other covering 6000 Å with 2.0 Å resolution.

Some properties of the shutter are useful in other applications: it is a single-shot closed-open-closed device; it is electrically triggerable with a reproducibility of 5 μs for an exposure time of 50 μs; the range of exposure times is currently 8–150 μs; its very simple shuttering action is applicable to a much wider range of wavelengths than electrooptic devices such as the Kerr and Pockels cells. It could also be used for time-isolation in conjunction with pulsed laser photography of luminous gases and plasmas.

IV. THERMAL BALANCING

The suppression of systematic errors in measuring the transition probabilities of lines emitted from a thermal light source must stem ultimately either from a greatly improved ability to specify the temperature of such a source (i.e., well beyond the currently feasible accuracy of order 2 percent) or from an operational trick which applies bounds (on the atomic level population) which are not available from today's imprecise temperatures alone. We have employed the latter method [1], [7] in a version called "thermally insensitive balancing," which can be applied to most spectral lines of atoms and ions because of the existence of reliable transition probabilities for a few lines such as H$_\beta$(HIλ4861) and NeIλ5852; the upper energies for these lines are 12.69 and 18.88 eV, respectively.

The transition probability A_{nm} for an optically thin line emitted with specific intensity I_{nm} from a homogeneous light source of length l is given by

$$A_{nm} = \frac{4\pi c I_{nm}}{h\lambda_{nm} l N_n} \tag{1}$$

where h is Planck's constant, c is the velocity of light, λ_{nm} is the wavelength of the line, and N_n is the number density of
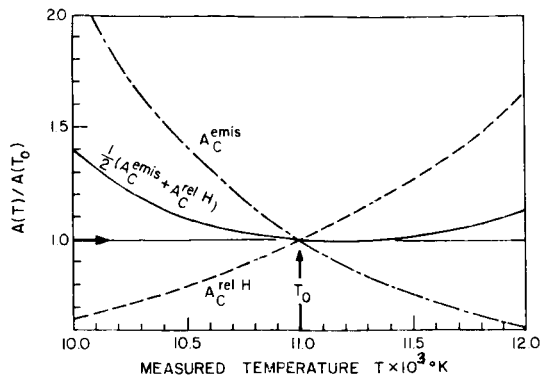
Fig. 4.   Relative error in measured A values of $Cl\lambda5052$ due to temperature errors. Chemical composition of the spectroscopic plasma is $\frac{1}{2}$ percent $CH_4 + \frac{1}{2}$ percent CS_2 + 99 percent neon and its pressure is 8.9 atm. A_C^{emis} is the value obtained by the conventional absolute emission technique, and $A_C^{rel\ H}$ is a measurement relative to H_β. By performing both determinations simultaneously, one obtains the thermally insensitive result $\frac{1}{2}[A_C^{emis} + A_C^{rel\ H}]$.

atoms (in the upper energy level E_n) responsible for the line emission. As well as other factors, N_n contains the Boltzmann factor, $\exp(-E_n/kT)$, which is responsible for the sensitive dependence of N_n upon plasma temperature T. Errors in T give rise to errors in N_n according to

$$\frac{\Delta N_n}{N_n} = \frac{E_n}{kT} \cdot \frac{\Delta T}{T} \tag{2}$$

so that systematic temperature errors are multiplied (by a factor usually of order 10) into systematic errors in N_n and, correspondingly, A_{nm}. Fig. 4 illustrates the thermal dependence (dashed curve labeled A_C^{emis}) of the A value for the line $Cl\lambda5052$—i.e., the A values one would obtain via (1) for different assumed temperatures T when the actual plasma temperature was T_0 (11 000°K in this case).

The figure also shows the opposite trend of A values ($A_C^{rel H}$) if one relates the carbon line intensity to a standard well-known line such as H_β via

$$A(Cl\lambda5052) = A(Hl\lambda4861)\frac{I_c}{I_{H_\beta}}\frac{\lambda_{H_\beta}}{\lambda_c}\frac{N_{H_\beta}}{N_c} \tag{3}$$

which tacitly assumes a known hydrogen-to-carbon ratio in the plasma and a complete thermodynamic calculation of of the plasma state. The factor N_{H_β}/N_c gives this curve a slope *opposite to* A_C^{emis} because the upper energy level for H_β lies *higher* above the hydrogen ground state than the carbon energy level of interest, reversing the sign of the argument of the Boltzmann function from the previous case. This curve levels out at high temperature only when extreme ionization of carbon offsets the growth of its Boltzmann factor relative to that of the H_β level in hydrogen.

Thermal balancing is achieved by averaging the results of the two methods in each experiment; the average curve is shown as solid in Fig. 4. It has a much lower slope than the other two curves, and lies almost entirely above the true A value in this range of operating temperature T_0. Thus the so-determined transition probability will be close to and not less than the true value, leaving aside random errors of photometry. As always, these errors require to be minimized

Fig. 5.   Summary of atomic data collected by the University of Maryland shock tube. Line shapes and line strengths can generally be measured in the same plasma. Data for the bracketed elements are presently being reduced.

in order to obtain the best precision; but the important and often systematic error in temperature, which has so often plagued A-value determination in the past, can be done away with by the proper choice of thermal balancing. For practically all atom and ion lines, and under a wide range of plasma conditions, one or two thermal balancing methods may be employed. For lines of ionized phosphorus, for example, the best choice is a "double relative" method [7] which averages the results obtained relative both to H_β and $Ne l\lambda5852$.

V. ATOMIC TRANSITION PROBABILITIES

A summary table of results for A_{nm} is given in Fig. 5. Many of the detailed results have been distributed in preliminary form [8]-[10] some have been published [11]-[14], and many are in final stages of preparation. This summary may be useful to anyone needing results for a particular species occurring in a plasma device, and it may be possible for us to obtain data for other atoms on request. New instruments are being tested which should extend our wavelength coverage to 1600 Å in the ultraviolet and 2.5 μ in the infrared. In any case, the Data Center on Atomic Transition Probabilities at the National Bureau of Standards should be consulted for comprehensive and up-to-date surveys of world data on atomic transition probabilities [15]. From (1) it should be clear that an experimenter possessing reliable A values for lines of a given element can determine the abundance of that element in a thermal radiating plasma if he knows both the temperature and pressure; moreover, the temperature itself can be measured, given the A value for a number of optically thin lines arising from a suitably wide range of energy levels [1]. Any continuum radiation underlying the lines must be subtracted beforehand, and is generally more easily recognized in photographic spectra than in photoelectric line measurements.

VI. STARK BROADENING PARAMETERS

The energy levels in an atom are perturbed by the application of an electric field, so that the atom's spectral lines are split into components. These components become blurred together in a dense plasma, owing to the statistical and time-varying nature of the local electric field around any atom or ion. The average line shapes can then be characterized by Stark broadening parameters which relate the width of the compound feature, and its shift relative to the zero-field wavelength, to the plasma electron density n_e.
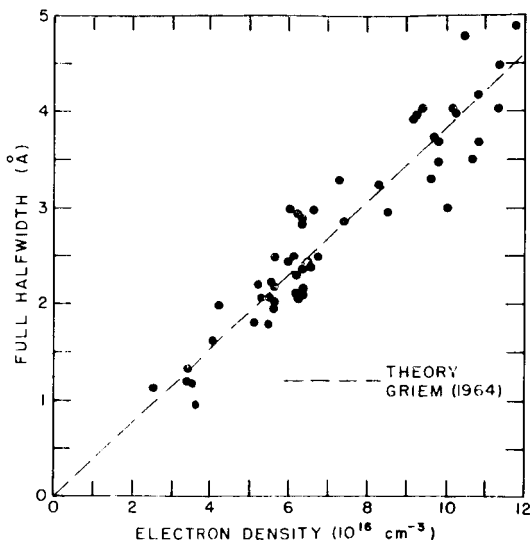
Fig. 6. Half intensity widths (FWHM) of Clλ5052 measured as a function of electron density. Predictions of the GBKO line broadening theory are also shown.

The experiments [16] summarized here have provided an extensive check on prior calculations [17], [18] of neutral line broadening and are now concentrating on the experimentally and theoretically more difficult subject of ion line broadening. A single spectrographic plate provides Stark shifts and widths for many lines recorded simultaneously at a single value of n_e; this in turn can be varied by nearly two orders of magnitude to check the functional relationship between n_e, line shift, and linewidth.

In every experiment, electron density is both *calculated* from pressure, temperature, and composition of the plasma and *measured* by means of the well-understood Stark broadening of the H$_\beta$ line [19]; these two results are identical to within 3 percent for n_e in the range 3–12 × 10^{16} cm^{-3}.

Results on Stark width are exemplified by Fig. 6, which summarizes sixty experiments on Clλ5052. For thirty five measured neutral lines, the expected linear relationships between n_e and linewidth, and between linewidth and shift, have been verified and the appropriate coefficients measured. The former proportionality agrees with Griem's prior calculations [17], [18] to within 8 percent. Nearly all of our data are concerned with relatively broad lines having high excitation potentials. If an experimenter must rely on such lines which are as yet unmeasured, provisional electron densities may therefore be obtained from Greim's neutral line calculations. The line shifts are smaller (and are, therefore, harder to use for measuring n_e) and uniformly agree with calculations to within 20 percent.

VII. General State Measurements

Fig. 7 lists the methods [2] we use for determining pressure, temperature, and (Section VI) electron density. Total pressure is measured with commercial quartz transducers located both in the end and side walls of the shock tube. Emission and absorption spectra are used to obtain independent temperatures for each shock tube experiment.

The first two methods based on *observed line intensity* for lines of *known transition probability* are equivalent to solving

STATE MEASUREMENTS IN THE SHOCK TUBE		
Pressure, quartz gauges, (7-35 atmos)	5%	
Temperature (9000-13000 °K)		
Absolute Intensity NeIλ5852	3%	
" " H$_\beta$	3%	
" " H$_\alpha$ core	3%	
Line reversal H$_\alpha$	2%	
Electron Density (2-20 ×10^{15}/cm^3)		
Calculate from measured p,T	10%	
Measure $\lambda_{1/2}$ (H$_\beta$)	15%	
Measure $\lambda_{1/2}$ (H$_\alpha$)	20%	

Fig. 7. Techniques simultaneously employed to overdetermine the state of spectroscopic plasmas. The characteristic tolerances apply to optically thin gases and must be relaxed when mean optical depths exceed 0.3.

(1) for the population N_n ($\propto$ exp ($-E_n/kT$)) of the upper energy level. In this case the temperature sensitivity of N_n (discussed in Section IV) can be used to advantage, particularly for the high-excitation line NeIλ5852. For all these methods the total pressure and gas composition must also be known, in order to divide out the obvious dependence of line intensity on chemical abundance. For the H$_\alpha$ (HIλ6563) method, a special treatment [3] is required by the peculiarities of the Stark broadening of this line.

The fourth listed technique of line reversal [21] is applied to H$_\alpha$ because the line is strong and easily observed in emission and absorption. Any strong line will suffice, in fact, and one need not know its transition probability. The calibrated flash lamp shown in Fig. 2 is fired during the time of interest behind the reflected shock, and a 3-channel monochromator records the flash as seen through the shock tube plasma in narrow wavelength channels located on, and to both sides, of the H$_\alpha$ line. Twice during the flash (whose *peak* brightness exceeds that of a blackbody at the shock tube temperature) the intensity in all channels is the same, namely, when the brightness of the lamp passes through the value equal to that of a blackbody at the temperature of the shock tube gas. At this "reversal point," a spectrogram would show a featureless continuous spectrum, devoid either of the emission lines seen from the shock tube alone or of the absorption lines one would record during the short interval (on the order of a microsecond) when the lamp temperature was higher than the shock tube temperature. Prior calibration gives the absolute brightness at the time of reversal and, hence, the temperature of the shock tube plasma.

Two methods not discussed here are particularly noteworthy for possible application to laboratory plasmas whether or not they are used for spectroscopic purposes; they would be valuable adjuncts to the methods we have used, and their diagnostic utility should be considered by any experimenter. One is the measurement of n_e by means of two-color optical interferometry [22]; the other is the determination of kinetic temperature by means of ultrasonic velocity-of-sound measurements [31].

Carnevale *et al.* found that the reversal temperatures and the sound speed temperatures agreed within 2 percent over the range 4500–6800° K used for their measurements of CrI transition probabilities. Likewise the temperatures measured [2] by our four methods described previously agree

to within 1.5 percent in the range 9000–13 000°K. Wood and Wilson [32] have also demonstrated the 4 percent agreement of various temperature measurements in their work on high temperature air (11 000–14 000°K).

Ample evidence exists for thermal equilibrium in shock tube plasmas, and a variety of methods is available to experimenters using the shock tube for fundamental and practical purposes. An example of the latter is given in the final section.

VIII. OPTICAL DEPTH OF URANIUM PLASMAS

By incorporating UF_6 in the shock tube test gas (up to 2 percent in neon) we have obtained quantitative data on the emissivity of uranium-containing plasmas from 2500 to 8500 Å in the temperature range 7500–12 000°K. The results bear directly on the design of gas-core, fission reactors for propulsion, and MHD power generation [33].

Existing fission reactors employ solid materials which limit the operating temperature to about 3000°K and below. By choosing instead to use a gaseous fuel and a gaseous working fluid, and *optical radiation* as the means of heat transfer between them, it is hoped to obtain working fluid temperatures of order 10 000°K. Increasing attention is being paid to this concept, in spite of the many design difficulties to be overcome, because of the potentially high operating efficiency of such devices and the relative simplicity with which self-sustaining fission reactions can be initiated compared to thermonuclear fusion.

Fig. 8 is an idealized representation of a gas-core reactor. Essential to its operation are sufficient *emissivity* of the fissioning plasma and *absorptivity* of the working fluid; without the latter, the anticipated optical radiation flux to an outer container is of order 10–100 $kW \cdot cm^{-2}$. The plasma itself must transport radiation well enough that one obtains adequate energy flux into the surrounding fluid without requiring such high fission fuel temperature, and therefore high containment pressure, that no practical container could be built. Calculations of uranium plasma opacity have been made [34], and the purpose of the shock tube experiments is to check these predictions over a portion of the density and temperature ranges which is consistent with theoretical assumptions. Though other species are present in the shock tube when the test gas is UF_6 plus neon, the closely spaced lines of uranium dominate the spectrum because the fluorine and neon lines are few in number, widely separated and much harder to excite. Many lines of UI and UII have been identified; at the highest temperature, UI disappears and other lines emerge which are probably due to UIII. Currently efforts are underway to catalogue these high temperature lines and to measure the Stark broadening parameters for a few of the strongest lines of UI and UII.

Fig. 9 reproduces both a photometric reduction of the shock tube spectrum (0.3 Å resolution below 6800 Å and 1.2 Å above) and a calculation of absorptivity made with the program of Parks *et al.* [34]. Experiment is normalized to theory at 5000 Å to show both the relative agreement above 4500 Å and the decrease in experimental emissivity
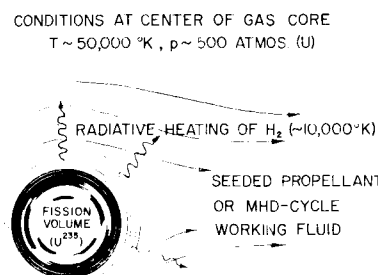
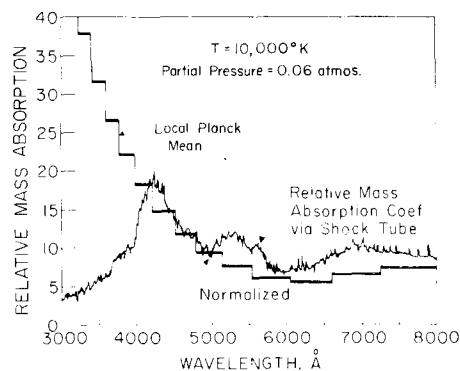Fig. 8. Principle of the gas-core fission reactor.

Fig. 9. Experimental and theoretical wavelength dependence of the absorption coefficient (3000–8000 Å) for a plasma temperature of 10 000°K and a uranium partial pressure of 0.06 atm.

compared to theory below 4200 Å. This is a typical result for all experiments, namely that they uniformly fail to show the predicted drastic rise in optical depth at shorter wavelength. In terms of net outward energy flux, this is a serious discrepancy between theory and experiment, because it takes place over that wavelength range where the gas Planck function is strongly peaked. The high predicted optical depth τ_v in this range would imply that the total flux $\int B_v(T)(1 - e^{-\tau_v})dv$ would be much higher than that obtained by similarly integrating with the observed optical depth.

As for sources of error, we have considered the following possibilities: 1) species such as F^- are present in the shock tube, which strongly absorb the uranium plasma radiation; this seems not to be the case since the implied absorption band does not correspond to the spectrum of any radical or molecule, and moreover the concentrations of such species are miniscule; 2) the theory does not account for important details of the dominant species UI and UII, since it is based on a scaled Fermi–Thomas statistical treatment of all uranium species which cannot properly represent autoionization, overlapping ionization continua, and the associated recombination radiation; this remains an open question for further research on the absorption spectrum of uranium vapor.

Fig. 10 summarizes for 5000 Å the dependence of optical depth on temperature and partial pressure of uranium. The dashed contour lines are taken from Parks *et al.*, and the cross-hatched regions show the shock tube observations. Two principal comparisons are evident: 1) observed emissivities are 2–5 times lower than predicted and 2) the logarithmic gradient of the optical depth in terms of the
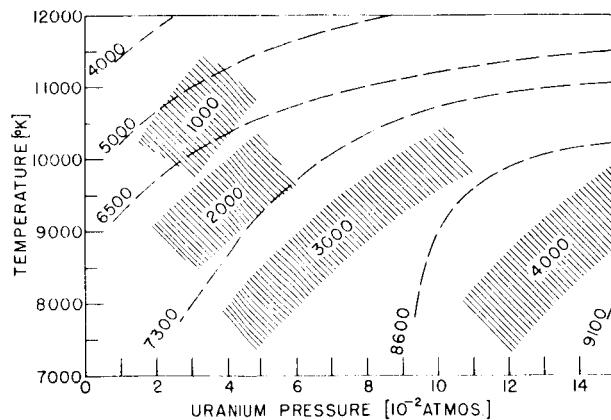
Fig. 10. Measured and predicted absolute optical absorption coefficients (5000 Å) for uranium as functions of temperature and uranium pressure. Curves are theoretically predicted contours of constant Planck mean capacity (cm²/g). Shaded areas represent measured mass absorption coefficients (cm²/g).

plotting variables is noticeably greater than predicted. Taken together with the discussion of Fig. 9, these results suggest that the sum total of the radiative processes active in uranium plasmas is not yet well enough understood to be calculated from first principles.

The experimental results seem useful in their own right over the range of variables so far studied. In order to improve the understanding of uranium plasmas, more effort is required on the ultraviolet spectrum, higher resolution at all wavelengths, and extending the ranges of temperature and pressure upward. In any case it will be important, in designing workable gas-core reactors, to obtain empirical emissivity data as close as possible to the operating pressure and temperature. The spectroscopic shock tube, previously employed for much lighter elements, has facilitated a quantitative start on this problem. An extension of the shock tube technique [36] to the generation of short-lived fissioning gases at high temperature may make it possible to approach more closely the physical conditions of interest.

REFERENCES

[1] T. D. Wilkerson, D. W. Koopman, M. Miller, R. Bengtson, and G. Charatis, "Atomic spectroscopy with the shock tube," *Phys. Fluids Suppl.*, vol. 12, 1969, pp. I-22 I-28. (*Proc. 6th Int. Shock Tube Symp.*)

[2] R. D. Bengtson, M. H. Miller, D. W. Koopman, and T. D. Wilkerson, "Comparison of measured and predicted conditions behind a reflected shock," *Phys. Fluids*, vol. 13, no. 2, Feb. 1970, pp. 372–377.

[3] M. H. Miller, and R. D. Bengtson, "A new method of absolute intensity calibration," *J. Quant. Spectr. Rad. Transfer*, vol. 9, Dec. 1969, pp. 1573–1578.

[4] S. M. Wood, and M. H. Miller, "A high speed spectrograph shutter," Maryland Univ., College Park, Md. Institute for Fluid Dynamics and Applied Mathematics, NASA Tech. Rep. CR-72660, March 1970, *Rev. Sci. Instr.*, vol. 41, no. 8, Aug. 1970, pp. 1196–1198.

[5] D. W. Koopman, "Computer programs for the calculation of equilibrium states in reflected shock plasmas," University of Maryland Tech. Note, BN-481, NASA Tech. Rep. CR-82931, Nov. 1966, pp. 1 58.

[6] R. A. Bell, R. D. Bengtson, D. R. Branch, D. M. Gottlieb, and R. Roig, "Computer programs for reduction of microphotometer data," University of Maryland Tech. Note, BN-572, NASA Tech. Rep. CR-105926, Oct. 1968, pp. 1 95.

[7] M. H. Miller, "A thermally insensitive technique for measuring atomic transition probabilities," *J. Quant. Spectrosc. Rad. Transfer*, vol. 9, Sept. 1969, pp. 1251–1259.

[8] ——, "Thermally insensitive determinations of transition probabilities for CI, OI, NeI, AlII, SiI, SiII, PI, PII, SI, SII and ClI," Ph.D. dissertation, University of Maryland Tech. Note BN-550, May 1968, pp. 1–318.

[9] R. D. Bengtson, "The measurement of transition probabilities and stark widths for CI, FI, NeI, ClI, ClII, BrI and BrII," Ph.D. dissertation, University of Maryland Tech. Note BN-559, July 1968, pp. 1–178.

[10] P. W. Murphy, "Krypton I line strengths: theory and experiment," Ph.D. dissertation, University of Maryland Tech. Note BN-523, Dec. 1967, pp. 1–126.

[11] M. H. Miller and R. D. Bengtson, "Relative transition probabilities for silicon," *The Astrophys. J.*, vol. 156, Apr. 1969, pp. 393–395.

[12] M. H. Miller, T. D. Wilkerson, and R. D. Bengtson, "Experimental SiI line strengths and their relation to solar abundances," *Bull. Amer. Astronom. Soc.*, vol. 2, no. 4, 1970, p. 331.

[13] R. D. Bengtson and M. H. Miller, "Experimental transition probabilities for neon I," *J. Opt. Soc. Amer.*, vol. 60, no. 8, Aug. 1970, pp. 1091–1096.

[14] R. D. Bengtson, M. H. Miller, D. W. Koopman, and T. D. Wilkerson, "Atomic transition probabilities of the halogens," *Phys. Rev., Ser. A*, vol. 3, Jan. 1971, pp. 16 24.

[15] W. L. Wiese, M. W. Smith, and B. M. Glennon, "Atomic transition probabilities," National Standard Ref. Data System, National Bureau of Standards Rep. NSRDS-NBS-4, Washington, D. C., 1966.

[16] M. H. Miller and R. D. Bengtson, "Measured Stark widths and shifts for neutral atomic lines," *Phys. Rev. Ser. A*, vol. 1, no. 4, Apr. 1970, pp. 983 990.

[17] H. R. Griem, M. Baranger, A. C. Kolb, and G. Oertel, "Stark broadening of neutral helium lines in a plasma," *Phys. Rev.*, vol. 125, Jan. 1962, pp. 177–195.

[18] H. R. Griem, *Plasma Spectroscopy*, New York: McGraw-Hill, 1964.

[19] P. Kepple and H. R. Griem, "Improved Stark profile calculations for the hydrogen lines H_α, H_β, H_γ and H_δ," *Phys. Rev.*, vol. 173, Sept. 1968, pp. 317 325.

[20] J. G. Clouston, A. G. Gaydon, and I. I. Glass, *Proc. Roy. Soc.* (London), vol. 248, 1958, p. 429.

[21] J. G. Clouston, A. G. Gaydon, and I. R. Hurle, *Proc. Roy. Soc.* (London), vol. 252, 1959, p. 143.

[22] G. Charatis, Ph.D. dissertation, University of Michigan, Ann Arbor, 1961.

[23] A. G. Gaydon and I. R. Hurle, in *Proc. 8th Int. Symp. on Combustion*, Baltimore, Md.: Williams and Wilkins, 1962.

[24] ——, *The Shock Tube in High Temperature Chemical Physics*, London, England: Chapman and Hall, 1963.

[25] A. R. Fairbairn, *Proc. Roy. Soc.* (London), vol. 267, 1962, p. 88.

[26] F. S. Faizullov, N. N. Sobolev, and E. M. Kudryavtsev, *Opt. i Spektroskop.*, 8, vol. 587, 1960, p. 761; [English transl.: *Opt. Spectrosc.*, (USSR), 1960, pp. 8, 311, 400].

[27] W. H. Parkinson and E. M. Reeves, *Proc. Roy. Soc.* (London), vol. 282, 1964, p. 265.

[28] G. Charatis and T. D. Wilkerson, *Phys. Fluids*, vol. 5, 1962, p. 1661.

[29] W. R. S. Garton, W. H. Parkinson, and E. M. Reeves, "Line-reversal measurements of excitation and electron temperature in a shock tube," *Proc. Phys. Soc.*, vol. 88, July 1966, pp. 771 773.

[30] R. A. Alpher and D. R. White, "Optical refractivity of high temperature gases, II: Effects resulting from ionization of monatomic gases," *Phys. Fluids*, vol. 2, March Apr. 1959, pp. 162 170.

[31] E. H. Carnevale, S. Wolnik, G. Larson, C. Carey, and G. W. Wares, "Simultaneous ultrasonic and line reversal temperature determination in a shock tube," *Phys. Fluids*, vol. 10, July 1967, pp. 1459 1467.

[32] A. D. Wood and K. H. Wilson, "Radiant energy transfer measurements in air," Lockheed Missiles and Space Co., Palo Alto, California; Rep. LMSC-681796, NASA Rep. CR-1390, NASA Oct. 1969, pp. 1 89.

[33] F. E. Rom, "Comments on the feasibility of developing gas core nuclear reactors," NASA Tech. Rep. TM-X 52644, 1969.

[34] D. E. Parks, G. Lane, J. C. Stewart, and S. Peyton, "Optical constants of uranium plasma," Gulf General Atomic, San Diego, Calif., NASA Contractor Rep. 72348, Final Rep., Feb. 1968, pp. 1 295.

[35] R. W. Patch, private communication (NASA-Lewis, Cleveland).

[36] W. N. Podney, Harold P. Smith, Jr., and A. K. Oppenheim, "Generation of a fissioning plasma in a shock tube," *Phys. Fluids, Suppl. 1*, vol. 12, *Proc. 6th Int. Shock Tube Symp.*, Apr. 1967, pp. I-68 I-72, 1969.